Author/s:
Kamei, KI;Koyama, Y;Tokunaga, Y;Mashimo, Y;Yoshioka, M;Fockenberg, C;Mosbergen, R;Korn, O;Wells, C;Chen, Y

Title:
Characterization of Phenotypic and Transcriptional Differences in Human Pluripotent Stem Cells under 2D and 3D Culture Conditions

Date:
2016-11-23

Citation:
Kamei, K. I., Koyama, Y., Tokunaga, Y., Mashimo, Y., Yoshioka, M., Fockenberg, C., Mosbergen, R., Korn, O., Wells, C. & Chen, Y. (2016). Characterization of Phenotypic and Transcriptional Differences in Human Pluripotent Stem Cells under 2D and 3D Culture Conditions. Advanced Healthcare Materials, 5 (22), pp.2951-2958. https://doi.org/10.1002/adhm.201600893.

DOI: 10.1002/ ((please add manuscript number))

Article type: Full Paper

Characterization of phenotypic and transcriptional differences in human pluripotent stem cells under two- and three-dimensional culture conditions

Ken-ichiro Kamei[1], Yoshie Koyama[1], Yumie Tokunaga[1], Yasumasa Mashimo[1], Momoko Yoshioka[1], Christopher Fockenberg[1], Rowland Mosbergen[2], Othmar Korn[2], Christine Wells[2,3], and Yong Chen[1,4*]*

Dr. K. Kamei [1], Dr. Y. Koyama [1], Y. Tokunaga [1], Dr. Y. Mashimo [1], M. Yoshioka [1], Dr. C. Fockenberg [1], and Prof. Y. Chen [1,4]

Institute for Integrated Cell-Material Sciences (WPI-iCeMS), Kyoto University, Kyoto 606-8501, Japan

E-mail: kkamei@icems.kyoto-u.ac.jp

This is the author manuscript accepted for publication and has undergone full peer review but has not been through the copyediting, typesetting, pagination and proofreading process, which may lead to differences between this version and the Version of Record. Please cite this article as doi: 10.1002/adhm.201600893.

This article is protected by copyright. All rights reserved.

Dr. R. Mosbergen [2,3], Dr. O. Korn [2], Prof. C. Wells [2,3]
Australia Institute for Biotechnology and Nanotechnology (AIBN), University of Queensland, Brisbane, QLD 4072, Australia

Department of Anatomy and Neuroscience, University of Melbourne, Melbourne, Vic, 3010, Australia

Prof. Y. Chen [1,4]

Ecole Normale Supérieure, CNRS-ENS-UPMC UMR 8640, 24 Rue L'homond, Paris 75005, France

E-mail: yong.chen@ens.fr

Keywords: human pluripotent stem cells, microfluidic device, hydrogel, three-dimensional cellular microenvironment, self-renewal

This article is protected by copyright. All rights reserved.

Human pluripotent stem cells (hPSCs) hold great promise for applications in drug discovery and regenerative medicine. Microfluidic technology is a promising approach for creating artificial microenvironments; however, although a proper three-dimensional (3D) microenvironment is required to achieve robust control of cellular phenotypes, most current microfluidic devices provide only 2D cell culture and do not allow tuning of physical and chemical environmental cues simultaneously. Here, we report a 3D cellular microenvironment plate (3D-CEP), which consisted of a microfluidic device filled with thermoresponsive poly(*N*-isopropylacrylamide)-β-poly(ethylene glycol) (PNIPAAm-β-PEG) hydrogel (HG), which enabled systematic tuning of both chemical and physical environmental cues as well as *in situ* cell monitoring. We showed that H9 hESCs and 253G1 hiPSCs in the HG/3D-CEP system maintained their pluripotent marker expression under HG/3D-CEP self-renewing conditions. Additionally, global gene expression analyses were used to elucidate small variations among different test environments. Interestingly, we found that treatment of H9 hESCs under HG/3D-CEP self-renewing conditions resulted in initiation of entry into the neural differentiation process by induction of *PAX3* and *OTX1* expression. We believe that this HG/3D-CEP system will serve as a versatile platform for developing targeted functional cell lines and facilitate advances in drug screening and regenerative medicine.

This article is protected by copyright. All rights reserved.

1. Introduction

Realizing the industrial, pharmaceutical, and clinical potential of human pluripotent stem cells (hPSCs; e.g., human embryonic stem cells [hESCs][1] and human induced pluripotent stem cells [hiPSCs][2]) requires derivation of the right cell type in an appropriate format for downstream applications. Current benchmarks in high-throughput screening do not include appropriate investigation of *in vivo* cell viability and do not adequately determine the capacity of hPSC-derived cells to functionally contribute to the target tissues.

One of the major barriers to obtaining the desired cellular phenotypes is establishing an appropriate cellular microenvironment.[3] This requires innovation in three areas: (i) identification and delivery of soluble factors, including growth factors, vitamins, chemical compounds, and bioactive gases; (ii) reconstitution of insoluble factors, such as extracellular matrix proteins, topological cues, shear stress, stiffness, pressure, and temperature; and (iii) factors facilitating cell-to-cell interactions, including gap junctions, tight junctions, and cellular adherence. In combination, these factors orchestrate the *in vivo* fate and function of cells with great precision. Most efforts directed at establishing a suitable microenvironment utilize only chemical cocktails of various soluble factors to drive cellular differentiation. Moreover, the current experimental settings rely on conventional macroscopic two-dimensional (2D) culture platforms, which lack precision and rely on the self-organizing ability of differentiating cells. Thus, these critical issues highlight the clear need to

This article is protected by copyright. All rights reserved.

experimentally establish appropriate *in vitro* cellular microenvironments that incorporate engineered three-dimensional (3D) systems, which can mimic well-organized *in vivo* tissue and cell regulatory systems.

Over the past decade, there has been a growing interesting in the application of microfluidic technology for the development of platforms to culture and treat cells and analyze cell functions, behaviors, and phenotypes in a robust, high-precision, and high-throughput fashion.[4] Indeed, such an approach holds many advantages over conventional cell culture methods, such as providing a configurable 3D space for cell culture, facilitating the control of small volumes of fluids, and allowing for integration of microelectromechanical systems (MEMSs) for sensing of cell components and behaviors. However, although some studies have performed 3D cell culture with established cell lines,[5] most hPSC studies have been performed in the 2D setting for maintenance of self-renewal,[6] controlled differentiation,[7] and enhanced reprogramming,[8] even in microfluidic cell culture chambers; to the best of our knowledge, no reports have described 3D cell culture and assays.[4b, 4c, 9] Therefore, the differences in hPSC behaviors in two- or three-dimensional culture conditions are still unclear. Without this knowledge, we will not be able to apply the optimal culture conditions for hPSCs for further differentiation procedures.

Here, we developed a simple microfluidic platform to create a 3D cellular environment using hydrogel for self-renewing hPSCs **(Figure 1A)**. We designated this device the 3D cellular environment

This article is protected by copyright. All rights reserved.

plate (3D-CEP). By combining the 3D-CEP device with a thermoresponsive poly(N-isopropylacrylamide)-β-poly(ethylene glycol) (PNIPAAm-β-PEG) hydrogel (HG), we were able to perform 3D hPSC culture within a microfluidic cell culture chamber. Finally, we elucidated the unique characteristics of each culture condition that influenced self-renewal and transcriptional networks.

2. Results and Discussion

2.1. Establishment of hydrogel-based 3D hPSC culture

We designed a 3D-CEP device having a cell culture chamber with a height of 200 μm to provide sufficient space for growth of cell aggregates. Previously, we reported a microfluidic device that could be used to generate concentration gradients of soluble cues, such as growth factors, to perturb hPSCs in hydrogel.[10] Compared with the previously reported device, the device developed in this study created more homogenous 3D culture conditions, since each channel was connected to two medium reservoirs to supply adequate cell culture medium and/or cellular stimulants. Moreover, this microfluidic channel also functioned as a container to maintain growing hPSC aggregates within the hydrogel. When hydrogel-based cell culture is performed in a conventional microtiter plate, the growing hPSC aggregates easily escape from the gel. However, using the microfluidic device, we could maintain the cells within the gel and minimize cell loss. The design incorporated a 0.75-mm-diameter inlet at the center of each microfluidic channel to facilitate loading of cells and HG. Polydimethylsiloxane

This article is protected by copyright. All rights reserved.

(PDMS) was used to fabricate the device because of its low cytotoxicity and good gas permeability.[6b, 11]

Moreover, we also used a 3D cellular matrix formed from a PNIPAAm-β-PEG hydrogel (HG, **Figure S1**) that was capable of temperature-induced phase changes at approximately 15°C, allowing the introduction, culture, and harvesting of cells in the 3D-CEP microfluidic device without additional reagents or cellular damage, which is challenging for other types of hydrogel, such as Matrigel, acrylamides, and other derivatives **(Figures 1B, S2, and S3)**.[10, 12] In this device, every cell in the culture was exposed to the same concentration of extrinsic soluble factors. mTeSR-1 medium[13] supplemented with 10 μM Y-27632 ROCK inhibitor[14] was used to culture the hPSCs and for dissolution of the HG. The optimal HG concentration for hPSC 3D culture was 61 mg mL^{-1} (**Figures S4–S11**). Therefore, these optimal conditions were referred to as "HG".

2.2. Phenotypic differences in hPSCs cultured under various conditions

Next, we examined the influence of cell culture conditions on the functional status of hPSCs **(Figures 2 and S4–S11)**. Conventional Matrigel-coated cell culture dish (MG)[13] and suspension (SP)[15] hPSC culture conditions served as experimental controls **(Figure 2A)**. In terms of morphology of the cell aggregates, H9 hESCs cultured for 4 days in HG exhibited

This article is protected by copyright. All rights reserved.

spherical cell shapes similar to SP-cultured cells. In contrast, the cells cultured under MG conditions formed a monolayer cellular sheet.

Cell viability after 4 days was assessed by monitoring intracellular adenosine triphosphate (ATP) production **(Figures 2B and S5)**. H9 hESCs cultured in HG, MG, and SP conditions did not exhibit variations in ATP production, thereby demonstrating the continued viability of the cells.

Cell aggregates that formed with culture under HG conditions were much smaller than those formed with culture under SP conditions **(Figure 2C)**. Under SP conditions, cells could freely move within the culture medium; therefore, they had more opportunity to aggregate with one another **(Movie S1)**. In contrast, HG-cultured cells were found to remain at a fixed location because of the elastic environment. This lack of cellular aggregation resulted in the formation of smaller cellular spheres **(Movie S2)**.

To quantitatively assess cell death, H9 hESCs were stained with annexin V and propidium iodide (PI), which are markers for apoptotic and dead cells, respectively, and were then subjected to flow cytometry **(Figures 2D, S6, and S7)**. Compared with MG conditions, SP and HG cultures showed increased numbers of annexin V-positive (p = 0.017 and 0.067, respectively), PI-positive (p = 0.0026 and 0.027, respectively), and double-positive cells (p = 0.03 and 0.08, respectively). These differences were attributed to the morphology of the cell aggregates. As mentioned previously, SP- and HG-cultured cells formed 3D spherical cell

This article is protected by copyright. All rights reserved.

aggregates, whereas MG-cultured cells formed 2D monolayer colonies. Therefore, soluble factors in the culture medium, such as growth factors, supplements, and gas molecules, did not reach the cells in the center of the 3D spherical cell aggregates. From a technical point of view, it is possible that dead cells in the MG cultures were washed away during daily changes in culture medium, thereby leading to underestimation of the number of apoptotic cells.

To characterize the effects of culture conditions on the cell cycle, flow cytometric analyses were performed for MG, SP, and HG conditions **(Figures 2E, S8, and S9)**. Compared with SP conditions, cells in HG cultures showed increased numbers of cells in the S phase (p = 0.042 determined by Student's t tests). As discussed above, cells in aggregate clusters have less opportunity to interact with soluble factors in the cell culture medium; therefore, cells in SP cultures exhibit fewer S-phase proliferating cells because of the formation of larger cell aggregate clusters than those in HG cultures.

2.3. Comparison of pluripotent marker expression

We evaluated the pluripotent status of hPSCs by performing immunocytochemistry and flow cytometric analysis **(Figure 3)**. H9 hESCs expressed the pluripotent stem cell markers octamer-binding transcription factor 4 (OCT4 [also known as POU domain, class 5, transcription factor 1 or POU5F1]) and NANOG **(Figures 3A and S10)**. Cell surface markers for pluripotency (stage-specific

This article is protected by copyright. All rights reserved.

embryonic antigen 4 [SSEA4] and TRA-1-60), but not differentiation (SSEA1), were highly expressed in H9 hESCs and 253G1 hiPSCs, and their expression did not differ among the culture conditions tested in this study **(Figures 3B and S11)**. These results also indicated that H9 hESCs cultured under HG conditions showed similar homogenous cellular populations as those cultured under MG and SP conditions. Expression levels of sex determining region Y-box 2 (*SOX2*), *NANOG*, and *OCT4* messenger ribosomal nucleic acid (mRNA) were also measured; these genes were highly expressed under all culture conditions in H9 hESCs, but not in IMR-90 human fibroblast negative controls **(Figures 3C–E)**. In summary, under the tested conditions, hPSCs maintained cell viability and pluripotent stem cell marker expression.

2.4. Influence of 3D cellular microenvironments on transcriptional networks

To identify the uniqueness of cellular function under each condition, we utilized microarray analysis techniques to investigate cellular gene expression profiles **(Figure S12)**.

First, we focused on the expression levels of the pluripotent stem cell markers *NANOG*, *SOX2*, and *OCT4* **(Figure 4A)**. For all culture methods, we observed similar gene expression levels (p = 0.95–0.99, as determined by moderated t-statistic tests); these gene expression levels were much higher than those observed in the IMR-90 fibroblasts, consistent with the stable pluripotency state in H9 hESCs under all tested conditions.

This article is protected by copyright. All rights reserved.

The culture microenvironment resulted in changes to gene expression, as illustrated by clustering of cells in the principle component analysis (PCA; **Figures 4B and S13**). To elucidate the biological pathways altered by each condition, we identified 253 genes differentially expressed among the HG, MG, and SP culture conditions (**Figure 4C**; $p < 0.05$ determined by moderated *t*-statistic tests).

Transcripts with similar expression patterns may be involved in the same pathways or similar functions; therefore, we used consensus clustering methods and attempted to categorize the transcripts by their expression patterns. Based on this analysis, five classes (classes 1–5) were identified **(Figures 4D and S14–S17)** containing 57, 61, 52, 45, and 38 transcripts, respectively. Classes 1 and 3 were downregulated under HG conditions as compared with that under MG and SP conditions. The other classes were upregulated under HG culture conditions **(Figures 4E and S14)**. We searched the gene ontologies for the transcripts in each class to determine their corresponding functions **(Figures 4F and S16-S17)**.

Transcripts exhibiting the class 1 expression pattern included genes from the metallothionein 1 family, such as *MT1L*, *MT1M*, *MT1E*, *MT1B*, *MT1G*, *MT1X*, and *MT1F*, which are associated with metal ion binding. These genes showed the highest level of expression in not only class 1 but also among all five classes. The metallothionein 1 gene expression and cell aggregate diameters have been reported to change according to the hydric environment of the culture method.[16] We observed similar variability in cultured cell

This article is protected by copyright. All rights reserved.

aggregate formation among MG, SP, and HG culture conditions in our experiments **(Movies S1 and S2)**.

Class 3 transcripts were associated with genes encoding neurotransmitter receptor activities (galanin receptor 1 [*GALR1*], cholinergic receptor nicotinic beta 4 [*CHRNB4*], cholinergic receptor nicotinic alpha 3 [*CHRNA3*], and sortilin-related VPS10 domain containing receptor 2 [*SORCS2*]) and regulation of neurogenesis (Forkhead box protein A1 [*FOXA1*], Von Willebrand factor C domain containing 2 [*VWC2*], and *CHRNA3*). This result indicated that cells cultured under HG conditions expressed the cell signals necessary to enter the later phases of neural differentiation.

Class 2 transcripts included genes related to the CXC family of chemokines (C-X-C motif ligand (*CXCL*) 5, *CXCL3*, and *CXCL2*). These CXC chemokines have a common receptor, CXC receptor 2 (CXCR2), which is associated with interferon (IFN)-γ-induced apoptosis in embryonic stem cells.[17] Both class 2 and class 4 transcripts were related to the Golgi apparatus and transmembrane proteins (bone marrow stromal cell antigen 2 [*BST2*], *CD44*, parathyroid hormone 1 receptor [*PTH1R*], adrenoceptor alpha 2A [*ADRA2A*], 5-hydroxytryptamine [serotonin] receptor 1D G protein-coupled [*HTR1D*], glucosaminyl [N-acetyl] transferase 1, core 2 [*GCNT1*], and major histocompatibility complex, class II, DQ alpha 1 [*HLA-DQA1*]), and most were related to the immune system. As shown in **Figure 2D**,

This article is protected by copyright. All rights reserved.

a slight increase in the number of apoptotic cells was observed in HG culture conditions, and the transcript analysis corroborated this observation.

Class 5 included seven transcription factors, e.g., diencephalon/mesencephalon homeobox 1 (*DMBX1*), *BTB* and CNC homology 1 basic leucine zipper transcription factor 2 (*BACH2*), orthodenticle homeobox 1 (*OTX1*), transcription factor AP-2 beta (*TFAP2B*), and paired box 3 (*PAX3*). PAX3 is involved in the early stages of neuron differentiation, and PAX3 and OTX1 are associated with forebrain development. Whereas the class 3 genes associated with neurotransmitter receptor activities and regulation of neurogenesis were downregulated, the class 5 genes associated with the early stages of neural differentiation were upregulated. In addition, as described above, the expression of genes associated with pluripotency did not differ among the tested SP, MG, and HG conditions. Thus, we hypothesized that, although hPSCs cultured under HG conditions maintained the expression of pluripotency markers, they initiated entry into the neural differentiation process.

3. Conclusions

In this study, we developed an HG/3D-CEP platform to carry out 3D hPSC culture for the first time. Global gene expression analyses provided mechanistic insights into the changes in gene networks resulting in phenotypic changes in the cells. The results of our study emphasized the importance of performing further investigations into the relationship between the culture microenvironment and cellular mechanisms.

This article is protected by copyright. All rights reserved.

Moreover, there is a growing interest in the development of organ-on-a-chip[18] and body-on-a-chip[19] devices to recapitulate human physiological and pathological conditions in vitro, and the combination of microfluidic and hPSC technologies is well suited to realize such devices for the preparation of collections of 3D differentiated and functional cells/tissues; however, the chips reported did not utilize 3D cell cultures. For example, primary hepatocytes from healthy donors would be a precious and functional resource but could lose their functions as hepatocytes after culture in conventional 2D cell culture dishes. Therefore, the cells on chips do not exhibit their correct functions; the findings obtained with such devices may not be relevant for real applications, such as drug screening and toxicological tests. Compared with conventional culture methods, including other microfluidics systems, our HG/3D-CEP platform enabled cells to maintain proper cell functionality and could be directly built into organ-on-a-chip and body-on-a-chip devices, which could have applications in future drug development. We believe that our HG/3D-CEP platform provides an important tool to facilitate the utilization of hPSCs in various clinical and industrial applications.

4. Experimental Section

Stereolithographic 3D printing of the microfluidic device: 3D-CEPs were fabricated using stereolithographic 3D printing techniques and solution cast molding processes **(Figure S1)**.[10] The mold for the microfluidic channels was produced using a 3D printer (Keyence Corporation, Osaka,

This article is protected by copyright. All rights reserved.

Japan). Sylgard 184 PDMS two-part elastomer (10:1 ratio of prepolymer to curing agent; Dow Corning Corporation, Midland, MI, USA) was well mixed and poured into a 3D-printed mold to produce a 5-mm-thick PDMS layer. The PDMS material was then cured in an oven at 65°C for 48 h. After curing, the PDMS form was removed from the mold, trimmed, and cleaned. The PDMS form and a glass dish or plastic plate were corona plasma-treated (Kasuga Denki, Inc., Kawasaki, Japan) and bonded together by baking in an oven at 80°C.

Culture of hPSCs in 2D mTeSR-1/MG and SP control conditions: Prior to culturing, Corning Matrigel hESC-Qualified Matrix (MG; Corning Inc., Corning, NY, USA) was diluted in a 1:75 v/v ratio with Dulbecco's modified Eagle medium (DMEM)/F12 (Sigma-Aldrich Corporation, St. Louis, MO, USA) and introduced into the culture dish. After 1 day of plate incubation in MG at 4°C, excess MG was removed, and the coated dish was washed with fresh DMEM/F12.

hPSCs were dissociated with TrypLE™ Express reagent (Thermo Fisher Scientific, Waltham, MA, USA) for 3 min at 37 °C and then harvested. A cell strainer was used to remove cell aggregates from the cell suspensions, and the cells were centrifuged at 200 × *g* for 3 min and then resuspended in mTeSR-1 medium. To prevent apoptosis of dissociated hPSCs, the mTeSR-1 medium was supplemented with 10 μM Rho-associated coiled-coil containing protein kinase (ROCK) inhibitor Y-27632 (Wako Pure Chemical Industries, Osaka, Japan) on day 1, and the medium was changed daily.

This article is protected by copyright. All rights reserved.

hPSCs cultured under MG conditions were counted using a NucleoCounter NC-200 cell counter (Chemometec A/S, Allerod, Denmark).

To establish the SP culture conditions, hPSCs cultured in Matrigel-coated dishes were dissociated using TrypLE Express. Cells were centrifuged at 200 × *g* for 3 min and resuspended in mTeSR-1 medium supplemented with 10 μM Y-27632. Dissociated cells were plated at an initial cell density of 2×10^4 cells cm^{-2} on Ultra Low Attachment Multiple plates (Corning Inc.) containing mTeSR-1 medium; the medium was changed daily. Cells were counted using a NucleoCounter NC-200 cell counter (Chemometec A/S).

hPSC 3D culture on 3D-CEP: Prior to use, 3D-CEPs were sterilized in 70% ethanol and placed under ultraviolet (UV) light in a biosafety cabinet for 30 min. hPSCs cultured on Matrigel-coated dishes with mTeSR-1 medium were trypsinized and collected in a 15-mL tube. Before loading of hPSCs, the 3D-CEP was placed on ice to maintain a low temperature. The dissociated hPSCs were resuspended in mTeSR-1 medium mixed with different concentrations of PNIPAAm-β-PEG hydrogel (HG; Mebiol Inc., Hiratsuka, Japan) supplemented with 10 μM Y-27632. HG concentrations of 45, 61, 76, and 91 mg mL^{-1} were utilized to obtain cellular matrices with stiffness properties identified as ultra-low, low, medium, and high, respectively. The hPSC/HG mixture was introduced into the 3D-CEP microfluidic device via a 0.75-mm-diameter inlet port. To promote gelation of the hPSC/HG mixture, the 3D-CEP was placed in a humidified incubator at 37°C in an atmosphere containing 5% CO_2. The mTeSR-1

This article is protected by copyright. All rights reserved.

medium was changed daily, and the HG concentrations were maintained within the range of 45 to 91 mg mL^{-1}, as determined by water solubility.

Cellular imaging: Cells were observed with an Eclipse Ti-E inverted fluorescent microscope system (Nikon Corporation, Tokyo, Japan) with a CCD camera (ORCA-R2; Hamamatsu Photonics K.K., Hamamatsu, Japan) and a CO_2 incubation chamber (Matsunami Glass Ind., Ltd., Osaka, Japan). During monitoring, the temperature of the incubation chamber was maintained at 37°C. To prevent evaporation of the samples, the inside of the chamber was kept in a highly humidified state.

Determination of PSC marker expression by flow cytometry: Cells were washed twice with phosphate-buffered saline (PBS) and harvested with TrypLE Express reagent. Cells were suspended in mTeSR-1/Matrigel culture medium and placed in 15-mL tubes. After centrifuging at 200 × *g* for 3 min, the supernatant was removed. Cells were washed twice with PBS, and then the cells were counted. For staining, the cells were diluted to 1×10^7 cells mL^{-1} in PBS supplemented with 2% (v/v) fetal calf serum (FCS). R-Phycoerythrin (PE)-labeled human anti-SSEA-4 antibodies (Stemgent, Cambridge, MA, USA), Dylight 488-labeled human anti-TRA-1-60 antibodies (Stemgent), and allophycocyanin (APC)-labeled human anti-CD15 (SSEA-1) antibodies (BioLegend, Inc., San Diego, CA, USA) were added to the cell suspensions and incubated at room temperature for 30 min.

This article is protected by copyright. All rights reserved.

Appropriate isotype-control antibodies were also used. Stained cells were centrifuged at 200 × *g* for 3 min, washed in PBS with 2% (v/v) FCS, and then loaded into a FACSCanto II cell analyzer (BD Biosciences, San Jose, CA, USA).

Global gene expression analysis: A total of 100 ng of RNA from each sample was amplified and labeled with cyanine 3 (Cy3) fluorescent dye to synthesize complementary viral RNA (cRNA) using a One-Color, Low Input Quick Amp Labeling Kit (Agilent Technologies, Santa Clara, CA, USA). Subsequently, 0.6 µg of synthesized cRNA was hybridized to SurePrint G3 Human GE 8×60K Ver.2.0 microarrays (Agilent Technologies). Data were analyzed with Stemformatics[20] and R/Bioconductors and normalized using the method described by Yugene.[21] The differentially expressed transcripts were identified and filtered using the statistical "Limma" linear modeling package ($p < 0.05$ and $q < 0.05$).[22] Consensus clustering was implemented in the *R* language using the ConsensusClusterPlus software package.[23] Functional gene classification was performed using the Database for Annotation, Visualization, and Integrated Discovery (*DAVID*) tool.[24] Data are available for download from #accession and Database or via http://www.stemformatics.org/datasets/search?ds_id=6153.

Quantitative reverse transcription polymerase chain reaction (RT-PCR) analysis: Total RNA was reverse transcribed using an RT^2 First Strand Kit (Qiagen, Hilden, Germany). cDNA was amplified and

This article is protected by copyright. All rights reserved.

quantified with the RT^2 SYBR Green ROX FAST Mastermix (Qiagen) in combination with an hESC-specific RT^2 Profiler PCR Array (PAHS-081Y; Qiagen). Data analysis was performed using Cluster 3.019 and Java TreeView 1.1.6r2 open source software.[25]

Supporting Information

Supporting Information is available from the Wiley Online Library or from the author.

Acknowledgements

Funding was generously provided by the Japan Society for the Promotion of Science (JSPS; 23681028 and 24656502). Funding was also provided by the Terumo Life Science Foundation. The WPI-iCeMS is supported by the World Premier International Research Centre Initiative (WPI), MEXT, Japan.

Received: ((will be filled in by the editorial staff))
Revised: ((will be filled in by the editorial staff))
Published online: ((will be filled in by the editorial staff))

This article is protected by copyright. All rights reserved.

[1] J. A. Thomson, J. Itskovitz-Eldor, S. S. Shapiro, M. A. Waknitz, J. J. Swiergiel, V. S. Marshall, J. M. Jones, *Science* **1998**, *282*, 1145-1147.

[2] a) K. Takahashi, K. Tanabe, M. Ohnuki, M. Narita, T. Ichisaka, K. Tomoda, S. Yamanaka, *Cell* **2007**, *131*, 861-872; b) J. Yu, M. A. Vodyanik, K. Smuga-Otto, J. Antosiewicz-Bourget, J. L. Frane, S. Tian, J. Nie, G. A. Jonsdottir, V. Ruotti, R. Stewart, Slukvin, II, J. A. Thomson, *Science* **2007**, *318*, 1917-1920; c) W. E. Lowry, L. Richter, R. Yachechko, A. D. Pyle, J. Tchieu, R. Sridharan, A. T. Clark, K. Plath, *Proc. Natl. Acad. Sci. USA* **2008**, *105*, 2883-2888.

[3] a) D. E. Discher, D. J. Mooney, P. W. Zandstra, *Science* **2009**, *324*, 1673-1677; b) D. Nampe, H. Tsutsui, *J. Lab. Autom.* **2013**, *18*, 482-493; c) S. W. Lane, D. A. Williams, F. M. Watt, *Nat. Biotechnol.* **2014**, *32*, 795-803.

[4] a) K. Kamei, *J. Lab. Autom.* **2013**, *18*, 469-481; b) O. Gagliano, N. Elvassore, C. Luni, *Biochem. Biophys. Res. Commun.* **2016**, *473*, 683-687; c) T. Qian, E. V. Shusta, S. P. Palecek, *Curr. Opin. Gene. Dev.* **2015**, *34*, 54-60; d) P. Ertl, D. Sticker, V. Charwat, C. Kasper, G. Lepperdinger, *Trends Biotechnol.* **2014**, *32*, 245-253; e) Z. Liu, X. Han, L. Qin, *Adv. Healthc. Mater.* **2016**, *5*, 871-888.

[5] a) S. G. Uzel, O. C. Amadi, T. M. Pearl, R. T. Lee, P. T. So, R. D. Kamm, *Small* **2016**, *12*, 612-622; b) Y. C. Chen, X. Lou, Z. Zhang, P. Ingram, E. Yoon, *Sci. Rep.* **2015**, *5*, 12175; c) G. Bergstrom, J. Christoffersson, K. Schwanke, R. Zweigerdt, C. F. Mandenius, *Lab Chip* **2015**, *15*, 3242-3249.

[6] a) L. G. Villa-Diaz, Y. S. Torisawa, T. Uchida, J. Ding, N. C. Nogueira-de-Souza, K. S. O'Shea, S. Takayama, G. D. Smith, *Lab Chip* **2009**, *9*, 1749-1755; b) K. Kamei, M. Ohashi, E. Gschweng, Q. Ho, J. Suh, J. Tang, Z. T. For Yu, A. T. Clark, A. D. Pyle, M. A. Teitell, K. B. Lee, O. N. Witte, H. R. Tseng, *Lab Chip* **2010**, *10*, 1113-1119; c) S. Giulitti, E. Magrofuoco, L. Prevedello, N. Elvassore, *Lab Chip* **2013**, *13*, 4430-4441.

[7] G. G. Giobbe, F. Michielin, C. Luni, S. Giulitti, S. Martewicz, S. Dupont, A. Floreani, N. Elvassore, *Nat. Meth.* **2015**, *12*, 637-640.

[8] C. Luni, S. Giulitti, E. Serena, L. Ferrari, A. Zambon, O. Gagliano, G. G. Giobbe, F. Michielin, S. Knobel, A. Bosio, N. Elvassore, *Nat. Meth.* **2016**, *13*, 446-452.

[9] D. Park, J. Lim, J. Y. Park, S. H. Lee, *Stem Cells Transl. Med.* **2015**, *4*, 1352-1368.

This article is protected by copyright. All rights reserved.

[10] K. Kamei, Y. Mashimo, Y. Koyama, C. Fockenberg, M. Nakashima, M. Nakajima, J. Li, Y. Chen, *Biomed. Microdev.* **2015**, *17*, 36.

[11] K. Kamei, Y. Hirai, M. Yoshioka, Y. Makino, Q. Yuan, M. Nakajima, Y. Chen, O. Tabata, *Adv. Healthc. Mater.* **2013**, *2*, 287-291.

[12] a) H. Yoshioka, M. Mikami, Y. Mori, E. Tsuchida, *J. Macromol. Sci. Pure* **1994**, *A31*, 121-125; bH. Yoshioka, M. Mikami, Y. Mori, E. Tsuchida, *J. Macromol. Sci. Pure* **1994**, *A31*, 113-120.

[13] T. Ludwig, V. Bergendahl, M. Levenstein, J. Yu, M. D. Probasco, J. Thomson, *Nat. Meth.* **2006**, *3*, 637-646.

[14] K. Watanabe, M. Ueno, D. Kamiya, A. Nishiyama, M. Matsumura, T. Wataya, J. B. Takahashi, S. Nishikawa, K. Muguruma, Y. Sasai, *Nat. Biotechnol.* **2007**, *25*, 681-686.

[15] R. Krawetz, J. T. Taiani, S. Liu, G. Meng, X. Li, M. S. Kallos, D. E. Rancourt, *Tissue Eng. C* **2010**, *16*, 573-582.

[16] H. Kempf, R. Olmer, C. Kropp, M. Ruckert, M. Jara-Avaca, D. Robles-Diaz, A. Franke, D. A. Elliott, D. Wojciechowski, M. Fischer, A. Roa Lara, G. Kensah, I. Gruh, A. Haverich, U. Martin, R. Zweigerdt, *Stem Cell Rep.* **2014**, *3*, 1132-1146.

[17] E. Tirotta, L. A. Kirby, M. N. Hatch, T. E. Lane, *Stem Cell Res.* **2012**, *9*, 208-217.

[18] a) M. W. van der Helm, A. D. van der Meer, J. C. Eijkel, A. van den Berg, L. I. Segerink, *Tissue Barr.* **2016**, *4*, e1142493; b) D. Bavli, S. Prill, E. Ezra, G. Levy, M. Cohen, M. Vinken, J. Vanfleteren, M. Jaeger, Y. Nahmias, *Proc. Natl. Acad. Sci. USA* **2016**, *113*, E2231-2240; c) W. Zhang, Y. S. Zhang, S. M. Bakht, J. Aleman, S. R. Shin, K. Yue, M. Sica, J. Ribas, M. Duchamp, J. Ju, R. B. Sadeghian, D. Kim, M. R. Dokmeci, A. Atala, A. Khademhosseini, *Lab Chip* **2016**, *16*, 1579-1586; d) B. Zhang, M. Montgomery, M. D. Chamberlain, S. Ogawa, A. Korolj, A. Pahnke, L. A. Wells, S. Masse, J. Kim, L. Reis, A. Momen, S. S. Nunes, A. R. Wheeler, K. Nanthakumar, G. Keller, M. V. Sefton, M. Radisic, *Nat. Mater.* **2016** *15*, 669-678; e) F. Zheng, F. Fu, Y. Cheng, C. Wang, Y. Zhao, Z. Gu, *Small* **2016**, *12*, 2253-2282; f) C. Oleaga, C. Bernabini, A. S. Smith, B. Srinivasan, M. Jackson, W. McLamb, V. Platt, R. Bridges, Y. Cai, N. Santhanam, B. Berry, S. Najjar, N. Akanda, X. Guo, C. Martin, G. Ekman, M. B. Esch, J. Langer, G. Ouedraogo, J. Cotovio, L. Breton, M. L. Shuler, J. J. Hickman, *Sci. Rep.* **2016**, *6*, 20030; g) F. An, Y. Qu, Y. Luo,

This article is protected by copyright. All rights reserved.

N. Fang, Y. Liu, Z. Gao, W. Zhao, B. Lin, *Sci. Rep.* **2016**, *6*, 25022; h) S. N. Bhatia, D. E. Ingber, *Nat. Biotechnol.* **2014**, *32*, 760-772.

[19] a) H. E. Abaci, M. L. Shuler, *Integr. Biol.* **2015**, *7*, 383-391; b) P. G. Miller, M. L. Shuler, *Biotechnol. Bioeng.* **2016** (DOI: 10.1002/bit.25989); c) S. H. Lee, S. K. Ha, I. Choi, N. Choi, T. H. Park, J. H. Sung, *Biotechnol. J.* **2016**; d) M. B. Esch, G. J. Mahler, T. Stokol, M. L. Shuler, *Lab Chip* **2014**, *14*, 3081-3092.

[20] C. A. Wells, R. Mosbergen, O. Korn, J. Choi, N. Seidenman, N. A. Matigian, A. M. Vitale, J. Shepherd, *Stem Cell Res.* **2013**, *10*, 387-395.

[21] K. A. Le Cao, F. Rohart, L. McHugh, O. Korn, C. A. Wells, *Genomics* **2014**, *103*, 239-251.

[22] a) G. K. Smyth, *Statistical applications in genetics and molecular biology* **2004**, *3*, Article3; b) G. K. Smyth, Y. H. Yang, T. Speed, *Meth. Mol. Biol.* **2003**, *224*, 111-136.

[23] M. D. Wilkerson, D. N. Hayes, *Bioinformatics* **2010**, *26*, 1572-1573.

[24] a) W. Huang da, B. T. Sherman, R. A. Lempicki, *Nat. Protoc.* **2009**, *4*, 44-57; b) W. Huang da, B. T. Sherman, R. A. Lempicki, *Nucl. Acids Res.* **2009**, *37*, 1-13.

[25] A. J. Saldanha, *Bioinformatics* **2004**, *20*, 3246-3248.

This article is protected by copyright. All rights reserved.

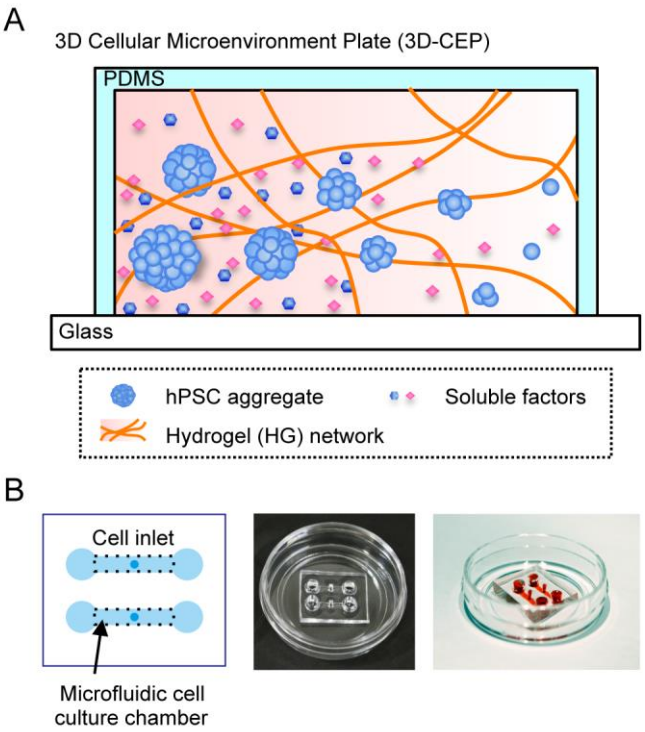

Figure 1. Microfluidic device to perform hydrogel-based three-dimensional (3D) hPSC culture, designated the 3D cellular microenvironment plate (3D-CEP). (A) Conceptual illustration of the 3D-CEP platform. By utilizing a thermoresponsive hydrogel (HG) mixed with soluble factors, 3D cellular microenvironments can be engineered within a microfluidic cell culture chamber. (B) Design of a 3D-CEP platform and representative photographs. The microfluidic cell culture chamber (10 mm [L] × 1.5 mm [W] × 200 µm [H]) had a total volume of 3 µL and was designed to connect with two different reservoirs (3 mm in diameter). The design incorporated a 0.75-mm diameter inlet at the center of each microfluidic channel to facilitate loading of cells and HG, allowing homogeneous cell culture.

This article is protected by copyright. All rights reserved.

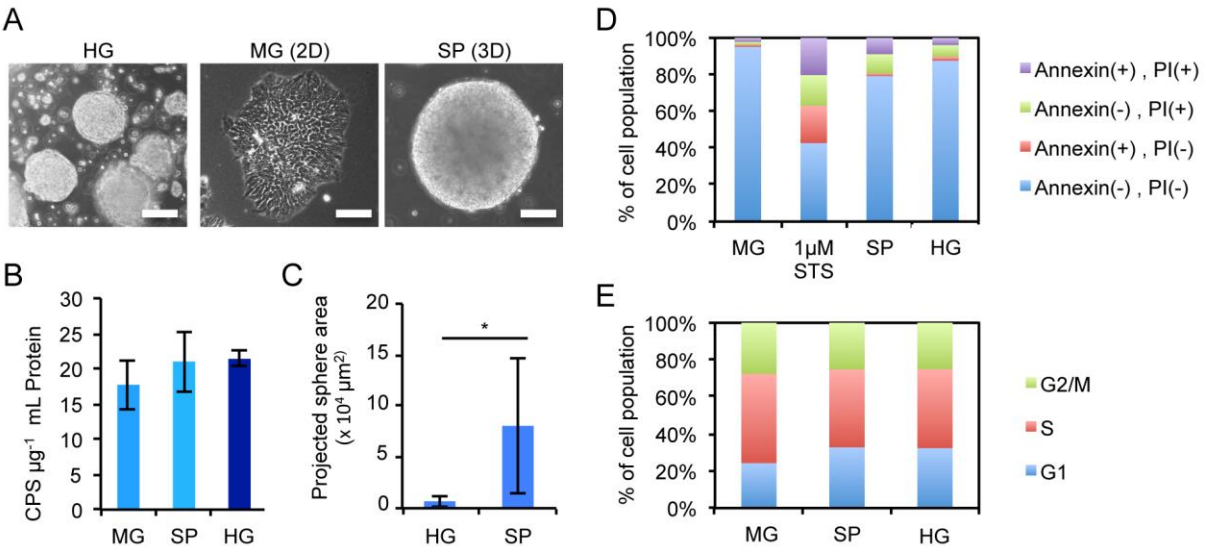

Figure 2. Evaluation of cellular status of H9 human embryonic stem cells (hESCs) cultured in 3D (e.g., HG and suspension [SP]) and 2D (Matrigel-coated cell culture plate [MG]) conditions. (A) Representative micrographs of H9 hESCs cultured in mTeSR-1 medium under HG, MG, and SP conditions. Scale bars represent 100 µm. (B) Intracellular ATP measurements to evaluate H9 hESC viability. Cell viability was determined by quantifying bioluminescence counts per second (CPS) of firefly luciferase in cell lysates (see Supporting Methods), and all data are represented as the mean ± SEM. There were no significant differences identified between the samples. (C) Comparison of the 2D-projected cell sphere sizes observed in HG and SP conditions (*$p = 7.8 \times 10^{-14}$). (D) Flow cytometric estimates of the percentage of dead H9 hESCs using apoptotic (annexin V) and dead cell (propidium iodide [PI]) markers. H9 hESCs cultured on Matrigel exposed to 1 µM straurosporine (STS) were used as a positive control for dead cells (see Supplementary Methods). The experiments were repeated five times. (E) Flow cytometric measurements of the cell cycle characterized by measuring nuclear contents of H9 hESCs using SYTOX AADvanced dye (see Supporting Methods). The experiments were repeated five times.

This article is protected by copyright. All rights reserved.

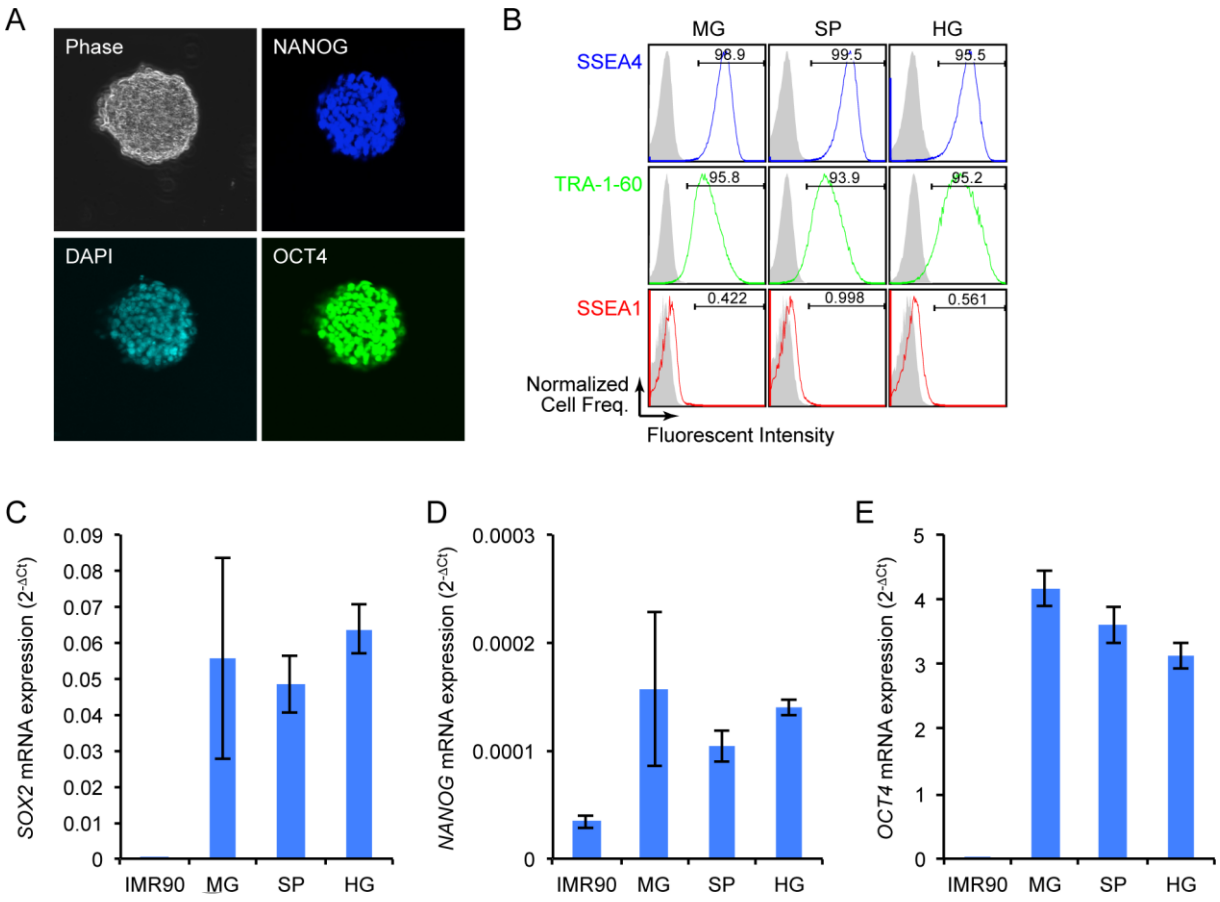

Figure 3. Comparison of the pluripotent status of H9 hESCs. (A) Whole-mount immunocytochemistry for OCT4 and NANOG expression in H9 hESCs in HG. (B) Flow cytometric analysis for pluripotency (SSEA4 and TRA-1-60) and differentiation (SSEA1) markers. (C–E) *SOX2*, *NANOG*, and *OCT4* mRNAs associated with pluripotency were measured using quantitative RT-PCR. As a negative control for pluripotent cells, human fetal fibroblasts (IMR-90 cells) were used (see Supporting Methods). All data are represented as the mean ± SEM, with n = 3.

This article is protected by copyright. All rights reserved.

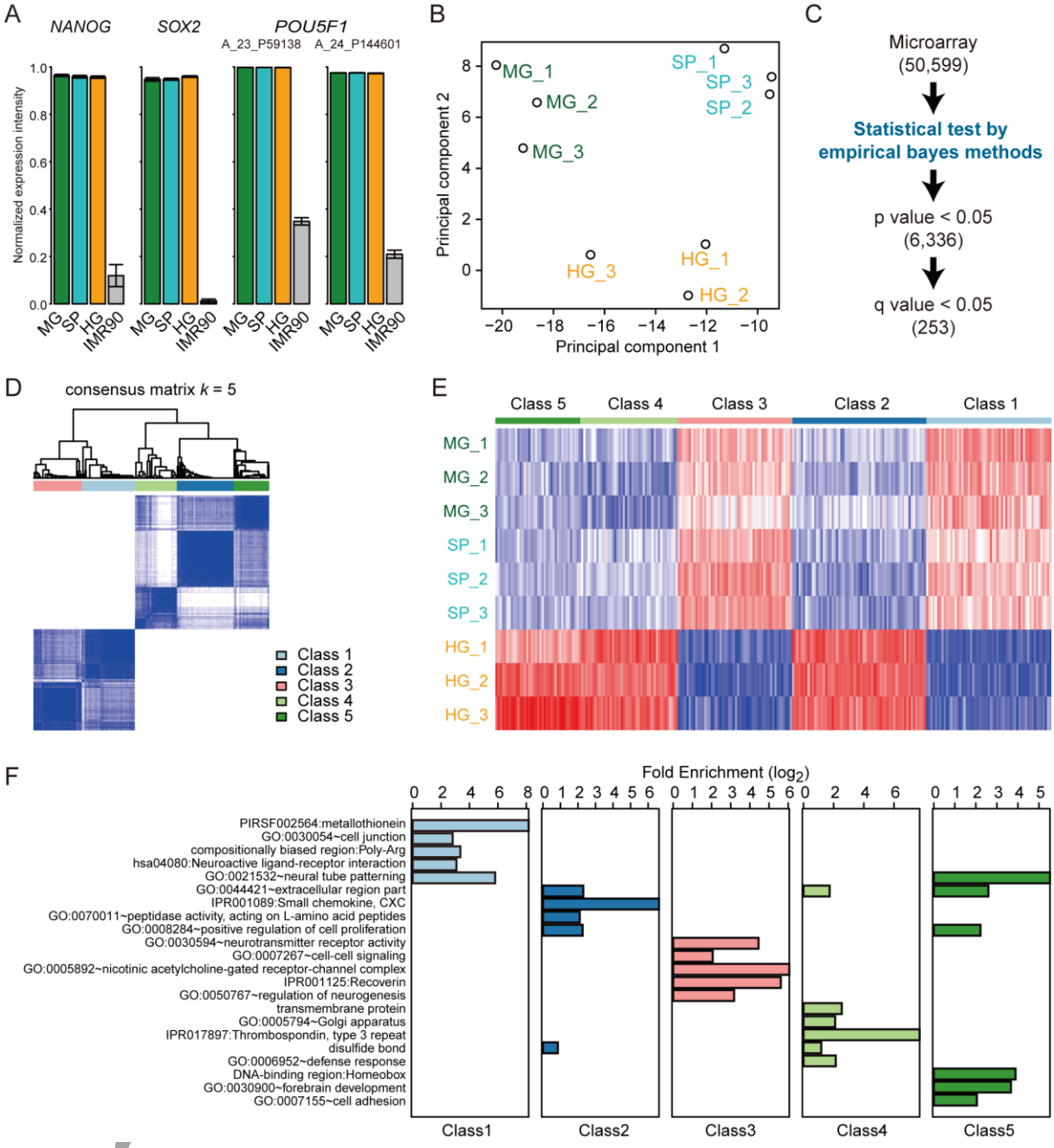

This article is protected by copyright. All rights reserved.

Figure 4. Comparison of gene expression signatures in H9 hESCs in the HG, MG, and SP conditions. (A) The expression levels of the pluripotent stem cell markers (e.g., *NANOG*, *SOX2*, and *OCT4* [or *POU5F1*]) in H9 hESCs did not differ among the tested microenvironments. As a negative control for pluripotent cells, IMR-90 cells were used. (B) Principal component analysis (PCA) based on microarray data showed that all HG (*orange*), MG (*green*), and SP (*light blue*) samples were segregated into three groups. (C) Workflow of the statistical filtering method used to identify differentially expressed gene transcripts. (D) Consensus clustering revealed that the identified transcripts were categorized into five classes. (E) Color-coded heat map for each consensus clustering class for the HG, MG, and SP conditions. (F) Gene ontological analysis for the functional annotation of the transcripts involved in each class.

This article is protected by copyright. All rights reserved.

A 3D cellular microenvironment plate (3D-CEP), which consists of a microfluidic device filled with thermoresponsive hydrogel (HG), for culture and analysis for human pluripotent stem cells (hPSCs). This HG/3D-CEP system enables culturing of hPSCs in a 3D fashion as well as *in situ* cell monitoring. Phenotypic and transcriptomic analysis of biological networks was performed after application of environmental cues.

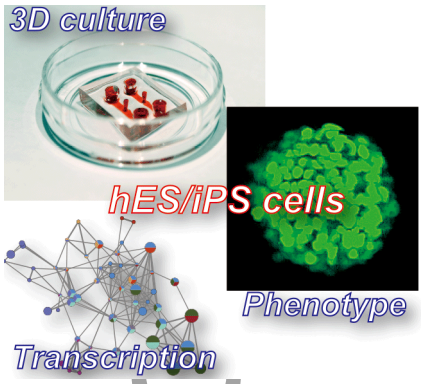

Keywords: human pluripotent stem cell; microfluidic device; hydrogel; three-dimensional cellular microenvironment; self-renewal

K. Kamei[1*], Y. Koyama[1], Y. Tokunaga[1], Y. Mashimo[1], M. Yoshioka[1], C. Fockenberg[1], M. Nakashima[1], R. Mosbergen[2], O. Korn[2], C. Wells[2,3], Y. Chen[1,4*]

Characterization of phenotypic and transcriptional differences in human pluripotent stem cells under two- and three-dimensional culture conditions

This article is protected by copyright. All rights reserved.